

Hyperpolarized ^{13}C MRI and PET: In Vivo Tumor Biochemistry

Ferdia A. Gallagher¹⁻³, Sarah E. Bohndiek^{1,2}, Mikko I. Kettunen^{1,2}, David Y. Lewis¹, Dmitry Soloviev¹, and Kevin M. Brindle^{1,2}

¹Cancer Research United Kingdom Cambridge Research Institute, Cambridge, United Kingdom; ²Department of Biochemistry, University of Cambridge, Cambridge, United Kingdom; and ³Department of Radiology, Addenbrooke's Hospital, University of Cambridge, Cambridge, United Kingdom

Dynamic nuclear polarization (DNP) is an emerging technique for dramatically increasing the sensitivity of magnetic resonance spectroscopy (MRS). This review evaluates the potential strengths and weaknesses of DNP-enhanced ^{13}C magnetic resonance spectroscopic imaging (DNP-MRSI) as a clinical imaging technique in comparison to PET. The major advantage of MRS is chemical shift, which enables the injected molecule to be observed separately from its metabolites, whereas the major advantage of PET is its high sensitivity. Factors such as spatial and temporal resolution and potential risks and costs of the two techniques will be discussed. PET tracers and ^{13}C -labeled molecules that can be used in oncology will be reviewed with reference to the biologic processes they detect. Because DNP-MRSI and PET are, in principle, similar techniques for assessing tumor metabolism, the experiences gained during the development of PET may help to accelerate translation of DNP-MRSI into routine patient imaging.

Key Words: animal imaging; molecular imaging; MRI; PET

J Nucl Med 2011; 52:1333–1336

DOI: 10.2967/jnumed.110.085258

PET techniques for imaging tumor metabolism have assisted the development of new drugs and been used to stage tumors and assess treatment response. Although used in a similar way, magnetic resonance spectroscopy (MRS) has not been widely adopted in the clinic, partly because of its poor sensitivity and other factors, such as interpretation. Dynamic nuclear polarization, or DNP (1), is a new technique that addresses this problem by significantly increasing the signal-to-noise ratio. Briefly, ^{13}C -labeled molecules, doped with small quantities of a stable radical, are cooled to approximately 1 K in a magnetic field; microwave irradiation transfers polarization from the fully polarized electron spins on the radical to the ^{13}C nuclei. The sample is then rapidly dissolved using a hot pressurized solution, which can be injected into an animal (or human) in a separate imaging magnet. The increase in signal-to-noise ratio with DNP-MRS is between 10^4 and 10^5 (Supplemental Fig. 1; supplemental materials are available online only at <http://jnm.snmjournals.org>), allowing detection not only of the substrate and products but also of their spatial distribution using spectroscopic

imaging (MRSI) (Fig. 1). The technique has been used to image ^{13}C -containing metabolites in tumors, cardiac tissue, and brain (2).

The first clinical trial of DNP-MRS is ongoing and is exploring the metabolism of hyperpolarized pyruvate in human prostate cancer. Consequently, it is important to consider what role it might play in the diagnosis and management of cancer patients, and its advantages compared with PET (Supplemental Fig. 1C shows a schematic of a clinical device (3)). The physical principles of the technique and its biomedical applications have been reviewed recently (2,4). Here, we compare the strengths and weaknesses of PET, DNP-MRS, and DNP-MRSI (Table 1).

SENSITIVITY

Sensitivity depends on many factors, including specific activity of the PET probe and concentration of the hyperpolarized substrate. However, despite the large increase in sensitivity afforded by DNP-MRS, PET is still much more sensitive; PET tracers can be detected in the nano- to picomolar range (5), whereas DNP-MRS sensitivity is still in the millimolar range. Therefore, hyperpolarized molecules are injected at concentrations that greatly exceed physiologic levels (e.g., 15–28 μmoles of pyruvate in mouse models (6,7)), whereas PET-labeled molecules can be administered at concentrations unlikely to perturb normal metabolism. An exception is hyperpolarized bicarbonate, which is already present at high concentrations in vivo (8); the ratio of hyperpolarized bicarbonate to carbon dioxide can be used to determine tissue extracellular pH.

MULTIPARAMETRIC DETECTION

The key advantage of DNP-MRS is that both the injected substrate and its metabolic products can be detected, allowing real-time observation of multiple metabolites. In addition, multiple hyperpolarized molecules can be detected simultaneously, allowing several metabolic pathways to be probed in conjunction with a marker of blood flow (9,10). In contrast, PET measures perfusion and accumulation of a tracer and does not differentiate between metabolites containing the radiolabel.

RANGE OF TRACERS AND TIMING OF ACQUISITION

For DNP-MRS, several requirements must be fulfilled for detection of metabolism in vivo (2); the ^{13}C -labeled molecule must be very soluble and there should be minimal spin–spin coupling to maximize polarization lifetime. Typically, this means the ^{13}C label must be in a carbonyl or carboxyl group. Nevertheless, polarization half-lives are typically only 10–30 s, and consequently, substrate injection and subsequent imaging must be accomplished within a few minutes. This requirement limits usable substrates to those that show relatively rapid metabolism,

Received Jun. 16, 2011; revision accepted Jul. 21, 2011.

For correspondence or reprints contact: Kevin M. Brindle, CRUK Cambridge Research Institute, Li Ka Shing Centre, Robinson Way, Cambridge, CB2 0RE, U.K.,

E-mail: kmb1001@cam.ac.uk

Published online Aug. 17, 2011.

COPYRIGHT © 2011 by the Society of Nuclear Medicine, Inc.

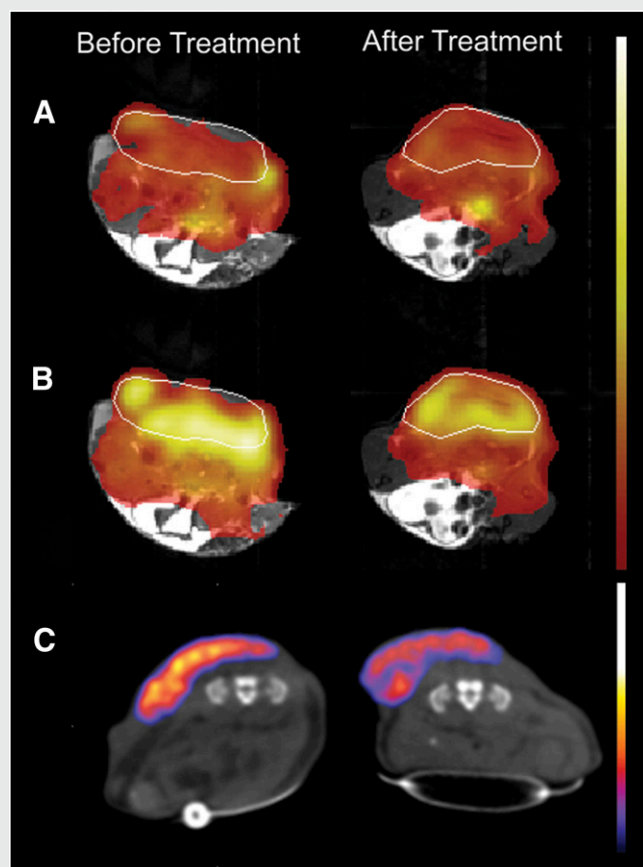


FIGURE 1. Comparison of $[1\text{-}^{13}\text{C}]\text{pyruvate}$ DNP-MRS and ^{18}F FDG PET in a murine lymphoma model. (A) Spatial distribution of injected hyperpolarized $[1\text{-}^{13}\text{C}]\text{pyruvate}$ before and 24 h after treatment of tumor-bearing animal with etoposide. Images were acquired from the same animal. Color maps of hyperpolarized $[1\text{-}^{13}\text{C}]\text{pyruvate}$ distribution are superimposed on gray-scale ^1H -MR images and have been normalized to mean pyruvate signal in tumor. Tumor margins are highlighted with a white line. (B) Spatial distribution of hyperpolarized $[1\text{-}^{13}\text{C}]\text{lactate}$ produced from injected hyperpolarized $[1\text{-}^{13}\text{C}]\text{pyruvate}$. Images are displayed using same scale as for pyruvate. (Reprinted with permission from (6).) (C) PET images acquired between 80 and 90 min after injection of 7 MBq of ^{18}F -FDG. Images were acquired before and after treatment, and color maps have been superimposed over gray-scale CT images. PET and DNP images were acquired from different animals.

with hyperpolarized $[1\text{-}^{13}\text{C}]\text{pyruvate}$ being the lead clinical candidate (4). Despite the restrictions for successful DNP-MRS, there are several promising ^{13}C -labeled molecules (Table 1). In contrast, there is a wide range of PET tracers, extending from labeled metabolites, such as ^{18}F -FDG, to labeled drugs (which are not in routine clinical use). Furthermore, although positron-emitting isotopes have relatively short half-lives, which limit human applications ($^{18}\text{F} = 109.7$ min; $^{11}\text{C} = 20.4$ min; $^{15}\text{O} = 2.04$ min, $^{13}\text{N} = 9.97$ min), these half-lives are much longer than those for hyperpolarization and therefore can be used to probe slower metabolism.

IMAGE ANALYSIS

Quantitative analysis of both PET and DNP-MRS generally requires pharmacokinetic modeling (6,11,12). A key difference with

DNP-MRS is that the lifetime of the label depends on various factors, such as the presence of paramagnetic centers. Consequently, it is difficult to derive absolute concentrations of the labeled molecules and thus to measure real fluxes (in mM/s); in most cases only rate constants for label flux are reported. Quantitative PET kinetic modeling can be simplified by correcting tracer concentration for injected dose and patient weight to produce a semiquantitative standardized uptake value. Similar approaches may be needed for clinical analysis of hyperpolarized substrate kinetics.

TEMPORAL AND SPATIAL RESOLUTION

Preclinically, the in-plane resolution of both techniques is comparable (1 mm), but PET can achieve an isotropic image resolution of about 1 mm, whereas DNP-MRSI often uses a thicker slice to improve signal-to-noise ratio (e.g., ~ 5 mm). However, DNP-MRSI can be acquired much more rapidly (<1 s) (4) and thus could be acquired within a single breath-hold, reducing motion artifacts. Clinically, the spatial resolution of PET is about 5 mm, and although the resolution of clinical DNP-MRSI is not yet known, with dedicated coils and pulse sequences, similar or better resolution should be achievable. PET can provide whole-body coverage, whereas DNP-MRSI is currently acquired over a limited field of view.

IMAGE COREGISTRATION

PET usually uses CT for anatomic coregistration. Although CT acquisition is rapid and relatively inexpensive, it results in additional radiation exposure and has reduced soft-tissue contrast when compared with ^1H -MRI. Administration of contrast medium greatly improves anatomic resolution but can complicate attenuation correction, although this effect is small. The recent introduction of combined PET/MRI will improve anatomic image contrast while providing further complementary information on tissue biology. For example, diffusion-weighted imaging may indicate whether reduced ^{18}F -FDG uptake was due to changed metabolism or a reduction in tumor cellularity. Hyperpolarized ^{13}C -MRSI will be performed in conjunction with ^1H -MRI, allowing diffusion-weighted imaging and other MR methods to be combined in the same patient examination.

RISKS

Current evidence suggests that the combined detriment from exposure to PET/CT radiation, due to excess cancer and heritable effects, is about 5% per sievert (13). Although these risks are small, they become important when multiple investigations are undertaken (e.g., to determine therapy response) and when children and women of reproductive age are imaged. The risks from MRI are largely secondary to the presence of ferromagnetic material inside or outside the patient. Magnetic fields per se, ^{13}C -enrichment, and hyperpolarization have no known biologic risks. However, although most hyperpolarized molecules are endogenous, they are injected at a high concentration and possible effects will need to be evaluated in dose-limiting toxicity studies.

COST AND AVAILABILITY

PET with ^{18}F -labeled molecules is widely available, and even many smaller hospitals have access to mobile PET scanners. Local ^{68}Ga generation may become available over the next few years. Few hospitals have an on-site cyclotron to enable the use of ^{11}C - and ^{15}O -labeled probes. Currently, clinical DNP-MRS is a research tool at a single site; however, since most hospitals in developed countries have access to MRI, and a sterile-use hyperpolarizer for potential clinical

TABLE 1
PET Tracers and DNP-Polarized Molecules with Clinical Imaging Potential in Oncology

Function	Molecule	PET or DNP	Biologic mechanism responsible for signal	Comments	Reference
Imaging cell death and treatment response	¹⁸ F-FDG	PET	Transported via glucose transporter Phosphorylated by hexokinase Measure of glucose utilization, glycolysis, and tumor cellularity	Leading PET tracer In routine clinical use Used for staging, monitoring treatment response, and detection of recurrence Can be used as specific biomarker of therapy response; for example, tyrosine kinase inhibition with imatinib	(14)
	[1- ¹³ C]pyruvate	DNP	Transported by monocarboxylate transporter Converted by lactate dehydrogenase into lactate Lactate signal dependent on endogenous lactate concentration as well as enzyme and coenzyme concentrations Binds to phosphatidylserine expressed on surface of apoptotic cells Also binds to phosphatidylserine on inner leaflet of plasma membrane bilayer during necrosis	Leading DNP substrate Preclinical marker of treatment response and tumor grade Clinical trials are beginning Can be used as specific biomarker of therapy response; for example, PI3K pathway inhibition Measures cell death Potential for early tumor detection and response to treatment	(6, 7, 10, 15, 16)
	¹⁹ F-annexin	PET	Binds to phosphatidylserine expressed on surface of apoptotic cells Also binds to phosphatidylserine on inner leaflet of plasma membrane bilayer during necrosis	Measures cell death Potential for early tumor detection and response to treatment	(17)
	¹⁸ F-isatin sulfonamide	PET	Binds to activated caspase-3/7	Measure of apoptosis Potential for early tumor detection and response to treatment Currently undergoing clinical trials	(18)
Imaging proliferation and cell growth	[1,4- ¹³ C ₂]fumarate	DNP	Hydrated by fumarase to form malate Transported into cell slowly, so significant metabolism is observed only in necrotic cells that have compromised plasma membrane integrity No coenzymes required	Noninvasive marker of necrosis in vitro and in vivo Marker of treatment response Low background signal No clinical data	(19, 20)
	3'-deoxy-3'- ¹⁸ F-fluorothymidine	PET	Thymidine analog Phosphorylated by thymidine kinase 1 Detects dividing cells	Marker of DNA synthesis and cell proliferation Potential for early detection of tumor response to treatment Kinetic modeling is required Ongoing multicenter clinical trials	(21)
	[5- ¹³ C]glutamine	DNP	Converted by intramitochondrial glutaminase into glutamate	Marker of glutamine metabolism, which may reflect cell proliferation Limited by short half-life of polarization and relatively slow metabolism	(22)
Imaging pH and hypoxia	¹⁸ F-fluoromisonidazole	PET	Nitroimidazole derivative Undergoes reduction and cellular trapping in hypoxic conditions	Marker of hypoxia	(23)
	⁶⁴ Cu-diacetyl-bis (N ⁴ -methylthiosemicarbazone)	PET	Reduction of Cu(II) to Cu(I) occurs in both normoxia and hypoxia but remains as Cu(I) in hypoxic conditions Cu(I)-ATSM is charged and trapped inside cell	Marker of hypoxia Potential marker of tumor aggressiveness Ongoing clinical trials Potential for use in radionuclide therapy	(23)
	[1- ¹³ C]pyruvate	DNP	See above	May report indirectly on hypoxia-inducible factor-1 (HIF-1)	(24)
	¹³ C-labeled bicarbonate	DNP	H ¹³ CO ₃ ⁻ exchanges with ¹³ CO ₂ rapidly, and ratio of the two is a measure of pH Exchange is almost instantaneous in presence of carbonic anhydrase	Measures extracellular pH predominantly	(8)
	⁶⁴ Cu pH low-insertion peptide	PET	Inserts into plasma membrane in presence of acidic extracellular environment	Measures relative extracellular pH	(5)

use has been described recently, the technique could become more widely applied (3) (Supplemental Fig. 1C). Although the running costs for DNP-MRS are currently unknown, it seems likely that they will be no more than for PET and could become cheaper as DNP-MRS becomes more widely available and the manufacturing of ^{13}C -labeled molecules increases.

CONCLUSION

There are a range of labeled molecules for probing tumor biology with PET and DNP-MRS (Table 1). However, PET is already established as a clinical tool and if DNP-MRS is to be adopted, it must provide complementary and clinically useful information. For example, DNP-MRS may provide additional patient information that could be used in conjunction with other imaging tests to assist in diagnosis and patient management. Furthermore, the quantitative information that DNP-MRS provides is of direct biologic relevance and could help further our understanding of tumor biology and accelerate new drug development.

Given the stringent requirements for a hyperpolarized molecule to be used in vivo, it is likely that only a limited number will be available for use in patients. Similarly, although there is a large number of PET probes, many centers use only one routinely: ^{18}F -FDG. Thus, the number of available tracers is not critical to success but rather the efficacy and biologic relevance of those that are available. The current leading DNP molecule is $[1\text{-}^{13}\text{C}]\text{pyruvate}$, and future research will determine whether it becomes the ^{18}F -FDG equivalent for DNP-MRS. It is likely to be used initially as an early treatment response marker and will have to demonstrate additional efficacy compared with that provided by ^{18}F -FDG. A second candidate molecule for clinical use is $[1,4\text{-}^{13}\text{C}_2]\text{fumarate}$, which has shown promise for detecting cell death.

The DNP-MRS community can learn from previous work undertaken in translating PET tracers to the clinic: the production of clinical-grade tracers, data modeling, and biologic validation are just a few examples of where the two techniques overlap. It has taken several decades for PET to gain widespread clinical acceptance, and studying the problems experienced with PET might help accelerate translation of DNP-MRS into a routine clinical imaging tool.

ACKNOWLEDGMENTS

We acknowledge Cancer Research U.K., the Leukemia and Lymphoma Society, the Wellcome Trust, the National Institute for Health Research Cambridge Biomedical Research Centre, and GE Healthcare for support. No other potential conflict of interest relevant to this article was reported.

REFERENCES

- Ardenkjaer-Larsen JH, Fridlund B, Gram A, et al. Increase in signal-to-noise ratio of $> 10,000$ times in liquid-state NMR. *Proc Natl Acad Sci USA*. 2003;100:10158–10163.
- Gallagher FA, Kettunen MI, Brindle KM. Biomedical applications of hyperpolarized ^{13}C magnetic resonance imaging. *Prog Nucl Magn Reson Spectrosc*. 2009;55:285–295.
- Ardenkjaer-Larsen JH, Leach AM, Clarke N, Urbahn J, Anderson D, Skloss TW. Dynamic nuclear polarization polarizer for sterile use intent. *NMR Biomed*. March 18, 2011 [Epub ahead of print].
- Kurhanewicz J, Vigneron DB, Brindle K, et al. Analysis of cancer metabolism by imaging hyperpolarized nuclei: prospects for translation to clinical research. *Neoplasia*. 2011;13:81–97.
- Culver J, Akers W, Achilefu S. Multimodality molecular imaging with combined optical and SPECT/PET modalities. *J Nucl Med*. 2008;49:169–172.
- Day SE, Kettunen MI, Gallagher FA, et al. Detecting tumor response to treatment using hyperpolarized ^{13}C magnetic resonance imaging and spectroscopy. *Nat Med*. 2007;13:1382–1387.
- Albers MJ, Bok R, Chen AP, et al. Hyperpolarized ^{13}C lactate, pyruvate, and alanine: noninvasive biomarkers for prostate cancer detection and grading. *Cancer Res*. 2008;68:8607–8615.
- Gallagher FA, Kettunen MI, Day SE, et al. Magnetic resonance imaging of pH in vivo using hyperpolarized ^{13}C -labelled bicarbonate. *Nature*. 2008;453:940–943.
- Wilson DM, Keshari KR, Larson PE, et al. Multi-compound polarization by DNP allows simultaneous assessment of multiple enzymatic activities in vivo. *J Magn Reson*. 2010;205:141–147.
- Witney TH, Kettunen MI, Hu DE, et al. Detecting treatment response in a model of human breast adenocarcinoma using hyperpolarized $[1\text{-}^{13}\text{C}]\text{pyruvate}$ and $[1,4\text{-}^{13}\text{C}_2]\text{fumarate}$. *Br J Cancer*. 2010;103:1400–1406.
- Zierhut ML, Yen YF, Chen AP, et al. Kinetic modeling of hyperpolarized C-13 (1)-pyruvate metabolism in normal rats and TRAMP mice. *J Magn Reson*. 2010;202:85–92.
- Watabe H, Ikoma Y, Kimura Y, Naganawa M, Shidahara M. PET kinetic analysis: compartmental model. *Ann Nucl Med*. 2006;20:583–588.
- ICRP. *Publication 103: Recommendations of the ICRP*. Amsterdam, The Netherlands: Elsevier; 2007.
- Collins CD. PET/CT in oncology: for which tumours is it the reference standard? *Cancer Imaging*. 2007;7 Spec No A:S77–S87.
- Day SE, Kettunen MI, Cherukuri MK, et al. Detecting response of rat C6 glioma tumors to radiotherapy using hyperpolarized $[1\text{-}^{13}\text{C}]\text{pyruvate}$ and ^{13}C magnetic resonance spectroscopic imaging. *Magn Reson Med*. 2011;65:557–563.
- Ward CS, Venkatesh HS, Chaumeil MM, et al. Noninvasive detection of target modulation following phosphatidylinositol 3-kinase inhibition using hyperpolarized ^{13}C magnetic resonance spectroscopy. *Cancer Res*. 2010;70:1296–1305.
- Yagle KJ, Eary J, Tait J, et al. Evaluation of F-18-annexin V as a PET imaging agent in an animal model of apoptosis. *J Nucl Med*. 2005;46:658–666.
- Nguyen QD, Smith G, Glaser M, Perumal M, Arstad E, Aboagye EO. Positron emission tomography imaging of drug-induced tumor apoptosis with a caspase-3/7 specific $[^{18}\text{F}]\text{-labeled isatin sulfonamide}$. *Proc Natl Acad Sci USA*. 2009;106:16375–16380.
- Bohndiek SE, Kettunen MI, Hu DE, et al. Detection of tumor response to a vascular disrupting agent by hyperpolarized ^{13}C magnetic resonance spectroscopy. *Mol Cancer Ther*. 2010;9:3278–3288.
- Gallagher FA, Kettunen MI, Hu DE, et al. Production of hyperpolarized $[1,4\text{-}^{13}\text{C}_2]\text{malate}$ from $[1,4\text{-}^{13}\text{C}_2]\text{fumarate}$ is a marker of cell necrosis and treatment response in tumors. *Proc Natl Acad Sci USA*. 2009;106:19801–19806.
- Bading JR, Shields AF. Imaging of cell proliferation: status and prospects. *J Nucl Med*. 2008;49(suppl 2):64S–80S.
- Gallagher FA, Kettunen MI, Day SE, Lerche M, Brindle KM. ^{13}C magnetic resonance spectroscopy measurements of glutaminase activity in human hepatocellular carcinoma cells using hyperpolarized ^{13}C -labeled glutamine. *Magn Reson Med*. 2008;60:253–257.
- Krohn KA, Link JM, Mason RP. Molecular imaging of hypoxia. *J Nucl Med*. 2008;49(suppl 2):129S–148S.
- Dafni H, Larson PE, Hu S, et al. Hyperpolarized ^{13}C spectroscopic imaging informs on hypoxia-inducible factor-1 and myc activity downstream of platelet-derived growth factor receptor. *Cancer Res*. 2010;70:7400–7410.
- Vävere AL, Biddlecombe GB, Spees WM, et al. A novel technology for the imaging of acidic prostate tumors by positron emission tomography. *Cancer Res*. 2009;69:4510–4516.



The Journal of
NUCLEAR MEDICINE

Hyperpolarized ^{13}C MRI and PET: In Vivo Tumor Biochemistry

Ferdia A. Gallagher, Sarah E. Bohndiek, Mikko I. Kettunen, David Y. Lewis, Dmitry Soloviev and Kevin M. Brindle

J Nucl Med. 2011;52:1333-1336.

Published online: August 17, 2011.

Doi: 10.2967/jnumed.110.085258

This article and updated information are available at:

<http://jnm.snmjournals.org/content/52/9/1333>

Information about reproducing figures, tables, or other portions of this article can be found online at:


<http://jnm.snmjournals.org/site/misc/permission.xhtml>

Information about subscriptions to JNM can be found at:

<http://jnm.snmjournals.org/site/subscriptions/online.xhtml>

The Journal of Nuclear Medicine is published monthly.
SNMMI | Society of Nuclear Medicine and Molecular Imaging
1850 Samuel Morse Drive, Reston, VA 20190.
(Print ISSN: 0161-5505, Online ISSN: 2159-662X)

© Copyright 2011 SNMMI; all rights reserved.

 SOCIETY OF
NUCLEAR MEDICINE
AND MOLECULAR IMAGING